JMEPEG (2012) 21:2002–2009
DOI: 10.1007/s11665-011-0112-0

1059-9495/$19.00

Influence of Al Contents on the Microstructure, Mechanical, and Wear properties of Magnetron Sputtered CrAlN Coatings

Hetal N. Shah and R. Jayaganthan

(Submitted December 2, 2010; in revised form August 5, 2011)

CrAlN ($0 < x < 0.1$) coatings were deposited on SA304 substrate by a reactive magnetron sputtering. The microstructure and composition of the as-deposited coatings were systematically characterized by field emission scanning electron microscopy/EDS and atomic force microscopy, and the phase formation by x-ray diffraction (XRD). The hardness of the coatings was investigated using nanoindentation, while wear properties were investigated using pin-on-disk tribometer. XRD study reveals that the deposited CrAlN coatings crystallized in the cubic B1 NaCl structure. The minimum and maximum hardness of the coatings are found to be 15.28 and 18.81 GPa, respectively. The COF and wear rate are found to be 0.48 and 2.25×10^{-5} mm^3/N·m, which is lower than the CrN coatings deposited and characterized under the same environment (0.63 and 2.25×10^{-5} mm^3/Nm).

Keywords CrAlN coatings, microstructure, Sputtering, wear

1. Introduction

Transition metal nitrides such as TiN, CrN, and HfN, with the NaCl (B1)-type lattice structure possess excellent tribological and chemical properties, which enable their use as wear resistant, corrosion resistant, and diffusion barrier coatings. The effect of additions of Al, Si, and Va on the mechanical and tribological properties of CrN coatings using cathodic arc ion plating (Ref 1, 2), cathodic arc evaporation (Ref 3), and DC/RF magnetron sputtering (Ref 4-8) has been reported in the literature. A significant increase in hardness value up to 30 GPa (Ref 4) to 35 GPa (Ref 9) or even higher values to 40 GPa (Ref 10) has been achieved for the CrAlN coatings when compared to CrN coatings. The coatings also exhibited higher thermal stability than pure CrN coatings.

Sun et al. (Ref 11) investigated CrAlN coatings deposited on different substrate materials such as Si (100), commercial aluminum alloy, AA6061, and M42 high speed steel (HSS). They found that the substrate material influences phase evolution in a reactively co-sputtered CrAlN films with Al contents favorable for B1 phase formation. Finally, they conclude that the B4 Wurtzite phase showed low hardness and poor ductility, which are not desirable for many industrial applications. A clustering of Al atoms in the B1 CrN (200) planes seems to occur, which leads to the large contraction of interplanar spacing for the films deposited on the HSS substrate. The coatings became more compact and denser, and the microhardness and fracture toughness of the coatings increased correspondingly with increasing substrate bias voltage (Ref 12). $Cr_{1-x}Al_xN$ coatings deposited on Si and stainless steel substrates using RF magnetron sputtering with different atomic concentrations of aluminum ($0.51 < x < 0.69$) showed the evolution of (111), (200), and (102) crystallographic orientations associated to the cubic $Cr_{1-x}Al_xN$ and w-AlN phases, respectively (Ref 13). The insertion of Al or AlN in the B1-type nitride coatings beyond solubility limits leads to phase transition from B1 to B4. Also, the solubility limit of AlN in B1 CrN has been calculated theoretically and found to be 77% as reported in the literature (Ref 14).

An incorporation of Al in to CrN coatings enhanced the tribological, oxidation, and mechanical properties as reported in the literature (Ref 2, 15-17) due to the formation of complex aluminum and chromium oxides, which prevents oxygen diffusion to the bulk (Ref 9, 18-21). It has been reported that PVD CrN coatings are deposited onto turning and milling tools for machining titanium and it alloys, where TiN coating is not suitable due to its strong adhesion (Ref 2, 15-17). With sufficient aluminum content ($Cr_{1-x}Al_xN$, $x > 0.2$) coating was found to be more oxidation resistant than CrN films (Ref 15). Wuhrer and Yeung (Ref 22) have made a comparative study of magnetron co-sputtered (Ti,Al)N and (Cr,Al)N coatings and reported that both the coatings followed similar development pattern (growth mechanism). The (Cr,Al)N coatings showed high deposition rate and hardness with increasing nitrogen pressure, suggesting its potential for many industrial applications in their work. The wear resistance of the $Cr_{1-x}Al_xN$ was dependent on Al and N concentrations in the films (Ref 23). The nanostructured CrAlN coating exhibited less material transfer and thus better adhesive wear protection than the TiN coating under both laboratory pin-on-disc tribo tests and industrial trial conditions (Ref 24).

Hetal N. Shah, Department of Metallurgical and Materials Engineering & Centre of Nanotechnology, Indian Institute of Technology-Roorkee, Roorkee 247667, India and Department of Mechanical Engineering, Sankalchand Patel College of Engineering, Visnagar 384315, India; **R. Jayaganthan**, Department of Metallurgical and Materials Engineering & Centre of Nanotechnology, Indian Institute of Technology-Roorkee, Roorkee 247667, India. Contact e-mail: rjayafmt@iitr.ernet.in.

A detailed investigation on the influence of microstructural characteristics of reactive magnetron sputtered CrAlN coatings on their mechanical properties, mainly hardness and modulus is limited in the literature. The transformation from B1 to B4 phase (Wurtzite structure) occurs in CrAlN coating, when the Al content is within the 51 to 69% (Ref 13) and it show comparatively lower hardness and modulus (Ref 11, 25) than the CrN coatings (B1 structure). The Al-rich coatings are more prone to oxidation than Cr-rich coatings and Cr/Al ratio of 0.9 offers the best resistant to oxidation (Ref 26), while in contrast, B4 phase has good oxidation resistance at high temperature (Ref 27). Owing to these facts, Al content in CrAlN coating has been fixed below 10 at.% in this study. The influence of Al content, $<10\%$ (within a solubility limit in B1 structure), on microstructural and mechanical properties of CrAlN coatings deposited by DC-reactive magnetron sputtering has been investigated in this study. The CrAlN coatings were characterized using the techniques such as XRD, FE-SEM/EDS, and AFM. The hardness was measured by microhardness tester while wear rate and coefficient of friction of the coatings were measured using pin-on-disc tribo tester in this study.

2. Experimental Procedure

CrAlN coatings were deposited on SA 304 steel (92 HRb) of 15×15 mm and 0.9 mm thick with a surface finish of 0.01 μm Ra using DC/RF magnetron sputtering (Model: DCSS-12, Manufactured by Excel Industries, Mumbai, India). Chromium target (cathode power fixed at 200 W) and aluminum targets (cathode power varied from 50 to 110 W) in a mixed Ar/N_2 atmosphere were used for the deposition of coatings. The Ar/N_2 flow ratio was maintained constant at 1:1, while the argon and the nitrogen flows set to value 10 sccm. The thickness of as-deposited coatings varied from 4.0 to 4.5 μm. The samples were ground, polished to an average surface roughness of <0.01 μm, and then cleaned with acetone in an ultrasonic container for 15 min. The samples were mounted on the rotational substrate holder cum heater and rotated in forward and reverse manner. The rotation angle were set (25°) in such a way that it covers maximum plasma region. Prior to deposition, the targets were sputter cleaned in Ar gas (1.33 Pa) for 10 min. The deposition parameters are summarized in Table 1.

The coating thickness was measured using its cross-sectional scanning electron micrographs. The microstructural and topographical analyses were made by field emission scanning electron microscopy (FESEM, Model: 200F, FEI Quanta) and atomic force microscopy (AFM, NTMDT). The composition of coatings was determined by the energy-dispersive x-ray (EDS) technique. The coatings were also analyzed by x-ray diffraction (XRD, Model: D8 Advance, Brucker), to determine the phase composition and orientation using a Ni-filtered CuKα x-ray source. The hardness of deposited CrAlN coatings was measured using microhardness tester (Miniload II, Leitz, Germany). The wear testing of coatings was performed with a pin-on-disc tribometer (Make: Magnum, Bangalore, India). The wear properties were obtained with the help of worn-out surface of pin and disc, wear debris and friction force produced during tribo test. The stainless steel (SA 304) pin was coated with CrAlN coatings and prepared with square configuration (7.5 to 7.5 mm), while EN 32 (65 HRC) material was used as a counter material. The normal load was kept constant, 10 N, with the relative sliding speed of 0.5 m/s during the test, which was carried out at room atmosphere in dry condition. The test was carried out for 2000 m sliding distance for all samples. The friction force between the deposited coatings and the counter material was measured, and divided by the normal load to calculate the friction coefficient. The observation of worn surface of coated pin was performed by a field emission scanning electron microscope (FESEM) and optical microscope (Model: Stemi 2000-C, Zeiss) with high-resolution Camera (SONY-Cybershot 4.1 mega pixels Model: DSC-585).

Table 1 Deposition condition for CrAlN coatings

Parameters	Value
Size of Cr and Al target	2″ (50.8 mm)
Substrate and substrate size	SA 304, $15 \times 15 \times 0.9$ mm
Substrate temperature	573 K
Gas environment and gas flow	$Ar + N_2$, 10 sccm
Working pressure	10 mTorr
Base pressure	4.0×10^{-6} Torr
Power	
Cr target	200 W fixed
Al target	50, 65, 80, 95, 110 W
Target to substrate distance	50 mm

To calculate the wear volume of the coated pin after testing, the profile of worn surface were measured at different locations using a profilometer and the average cross-sectional areas (A) of the worn tracks were determined. The wear rates (W) were obtained by following relationship (Ref 28):

$$W = \frac{\pi dA}{LN} \quad \text{(Eq 1)}$$

where d is diameter of wear track, L is total sliding distance, and N is load applied.

3. Result and Discussion

3.1 Effect of Al Content on Phase Composition of CrAlN Coating on SA304 Substrate Material

The XRD patterns of the $Cr_{1-x}Al_xN$ coating deposited on SA304 substrates with various values of Al content is shown in Fig. 1. It is shown that the coatings are highly textured with domination peak of CrN(111) with position being shifted to higher 2θ angle, with increasing Al content in the coating deposited on SA304. The peak shift in 2θ peaks in $Cr_{1-x}Al_xN$ coating may be due to substitution of Cr atoms by smaller Al atoms in CrN lattice (Ref 5, 29). The peak shifting to higher diffraction angle indicates a reduction in d spacing and lattice constant and vice versa, as shown in Table 2. Also, the reduction in lattice constant may indicate the possibility of formation of hexagonal, h-AlN (004) reflection as reported by Ding et al. (Ref 30). The actual solubility limit of Al in the coatings depends on the deposition conditions and the solubility of AlN in cubic CrN is as high as 77 mol%, the saturated CrAlN phase is thermodynamically metastable (Ref 31-33). The one diffraction peak corresponding to B1 CrAlN was detected from coated SA 304 substrate. There is no appreciable peak separation found within the range of applied power to the Al target as reported by the Li et al. (Ref 7). Also, there is no peak between 45° to 75° diffraction angle. Only one highly

textured peak corresponding to CrN(111) position with weak CrN(200) orientation is observed from the XRD results instead of two high intensity peaks corresponding to CrN(111) and CrN(220) orientations reported in the literature (Ref 11). It may be because of the higher nitrogen content during deposition and higher thickness of coating, which favors (111) plane due to the influence of strain energy (Ref 34-36). The lattice constant is calculated from CrAlN(111) peaks for coating deposited on SA304 substrate. The lattice constant a and lattice microstrain ε were calculated using Eq 2 and 3 (Ref 37-39).

$$\frac{1}{d^2} = \frac{h^2 + k^2 + l^2}{a^2} \quad \text{(Eq 2)}$$

where d is the interplanar distance obtained from the position of the (111) peak using the Bragg condition, and

$$\varepsilon = \frac{a - a_0}{a_0} * 100 \quad \text{(Eq 3)}$$

where a is the lattice constant in the strained condition and a_0 is the unstrained lattice constant (4.140 Å). The lattice constants were found to be decreasing with increasing Al content as shown in Table 2.

It has been reported in the literature (Ref 40) that the microstress increases with the deposition rate and hence coating thickness, because of the distortion of crystal lattice of the coating due to the comparatively high kinetic energy of the incident ions. The CrAlN coatings were deposited at the same temperature (573 K), and therefore thermal stresses of all the coatings were presumed to be the same in this study. The grain size and deposition rate of CrAlN coating as a function of Al content is shown in Fig. 2. It was found that with the incorporation of Al atoms in to the CrN coatings, the full width at half maximum (FWHM) of the CrN (111) diffraction peak is increased, and hence there is a reduction in grain size in the CrAlN coating. The FWHM and the microstrain as a function of Al content in CrAlN coating is shown in Fig. 3.

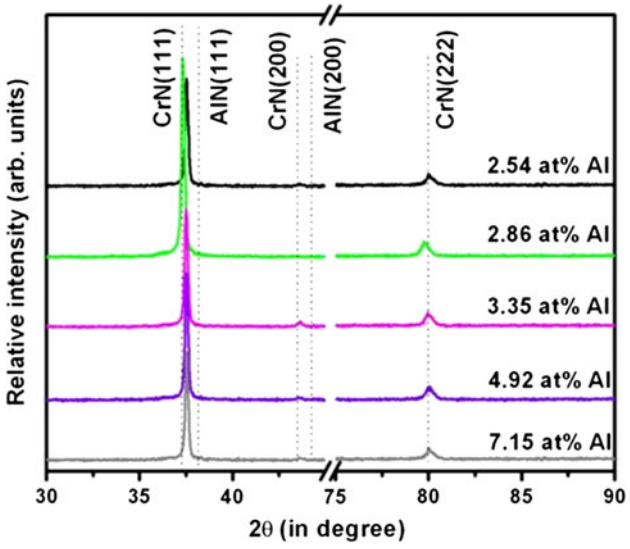

Fig. 1 X-ray diffraction profiles of the as-deposited coating prepared with different Al contents by magnetron sputtering on SA304 substrates

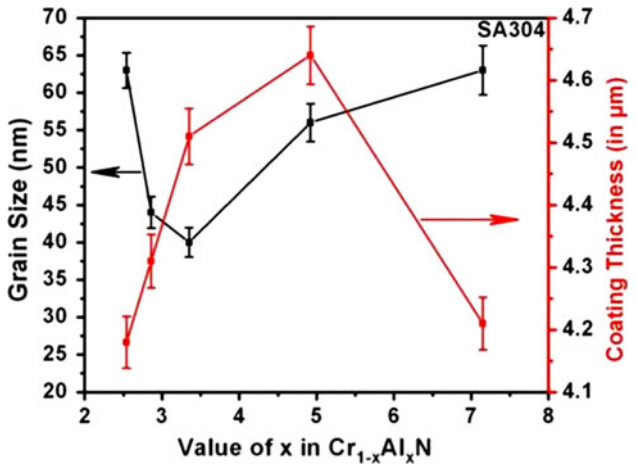

Fig. 2 Grain size and coating thickness as a function of Al content in the CrAlN coating

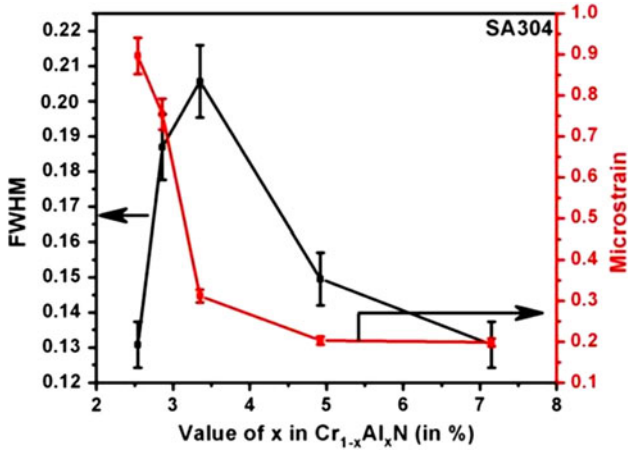

Fig. 3 FWHM and microstrain as a function of Al content in CrAlN coating

Table 2 Calculated FWHM, *d* spacing, lattice constant, and lattice microstrain as a function of Al content of CrAlN coating deposited on SA304 substrates

Sample	FWHM	*d* spacing	Lattice constant *a* for (111) orientation	Microstrain $\varepsilon = (a - a_0)/a_0$
CrAl(2.54 at.%)N	0.1308	2.4117	4.1771	0.8961
CrAl(2.86 at.%)N	0.1869	2.4083	4.1712	0.7536
CrAl(3.35 at.%)N	0.2056	2.3977	4.1529	0.3115
CrAl(4.92 at.%)N	0.1495	2.3951	4.1484	0.2028
CrAl(7.15 at.%)N	0.1308	2.3950	4.1482	0.1980

The CrAl(3.35 at.%)N coating shows a minimum grain size due to its comparatively higher deposition rate (75 nm/min). Due to this, the FWHM of CrAl (3.35 at.%)N, should be higher because of lower grain size. The lattice microstrain of the CrAlN is reducing with Al content and at CrAl(3.35 at.%)N, a lower microstrain value is observed despite its comparatively higher deposition rate. It is evident from the Fig. 3 and 4 that the microstrain of CrAl(3.35 at.%)N is reducing with coating thickness. The reduction in lattice microstrain is due to the formation of c-AlN (Ref 7). The high residual stress is responsible for phase separation of c-AlN from CrAlN. The relaxation of the lattice microstrain might occur during the phase separation. Two-dimensional surface topography of CrAlN coatings deposited at different Al contents were characterized using AFM and the morphology of the films was obtained using FE-SEM (Fig. 5). The coating becomes more compact and denser as seen in these micrographs. The overall roughness of the coating deposited on SA304 substrate is summarized in Table 3. The surface roughness is reducing with increasing Al content. The reduction in surface roughness and high density of the coating may be due to increasing, applied voltage to Al target, which may increase mobility of the atoms and results in higher nucleation density (Ref 41) during the formation of denser coating. The high mobility of the adatoms can move in to inter-granular voids and diffuse in the films. Higher nucleation density helps to produce denser coating and atoms with high mobility diffuse in to the intern granular voids (Ref 42, 43). The measured microhardness is found to be increasing with increase in Al content as shown in Fig. 6.

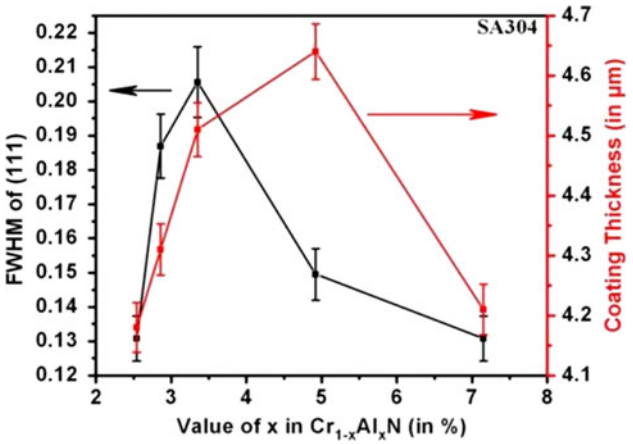

Fig. 4 FWHM and coating thickness as a function of Al content in CrAlN coating

Table 3 Grain size, surface roughness, and hardness of CrAlN coating at different Al contents deposited on SA304 substrate

Samples	Grain size (XRD, nm)	Roughness, nm		Deposition rate, nm/min	Hardness, GPa
		RMS	Av		
CrN	70	21	18	67	13.93
CrAl(2.54 at.%)N	63	10.34	8.28	70	15.28
CrAl(2.86 at.%)N	44	9.71	7.76	72	15.94
CrAl(3.35 at.%)N	40	10.09	7.99	75	16.95
CrAl(4.92 at.%)N	56	8.31	6.68	78	17.56
CrAl(7.15 at.%)N	63	9.08	7.17	70	18.81

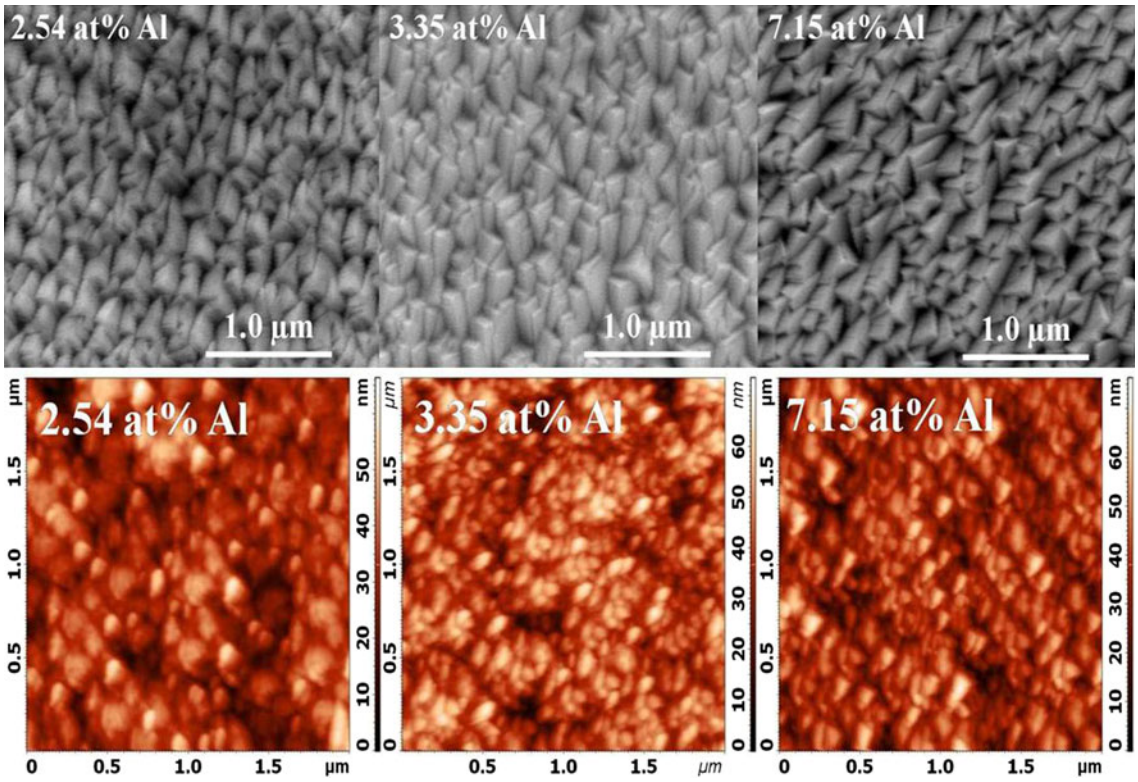

Fig. 5 FESEM and AFM images of CrAlN coating deposited on SA304 as a function of Al content

3.2 Wear Properties

When coated pin slides against steel disc (with surface roughness below 100 nm), the behavior of the material was highly influenced by the differences in hardness between the coated pin and the disc. As can be seen in Fig. 7, the EN 32 steel (65 HRC) was severely worn by coatings with high hardness, i.e., the CrN and the CrAlN coated pin. The wear test parameters are given in Table 4. During the pin-on-disc test of CrN coating, (Fig. 8) initially, the friction force was found to be around 4 to 5 N up to 5 minutes. Similarly, in the CrAlN coating, the friction force was observed to be around 2.0 to 3.0 in initial time. Subsequently, it is increased with sliding distance, which is purely attributed to the lower surface roughness of pin as well as disc and a counterpart, below 10 and 100 nm, respectively. It may be due to the perfect surface asperity contact of sample. After 2 to 3 minutes, friction force is increased suddenly to a range of 5 to 8 N (for CrN) and 4 to 6.5 N (for CrAlN) in the next 5 to 7 min following the generation, breaking and agglomeration of wear particles between pin and disc. Finally, it reaches to a steady state condition and becomes stable around 6.5 and 4.5 N for CrN and CrAlN, respectively, when the friction was governed by the viscous shearing of the coating (Ref 44). The calculated Hertzian contact pressure, minimum and maximum was 1.1 and 1.66 GPa, respectively, for the contact area of CrN and CrAlN coating.

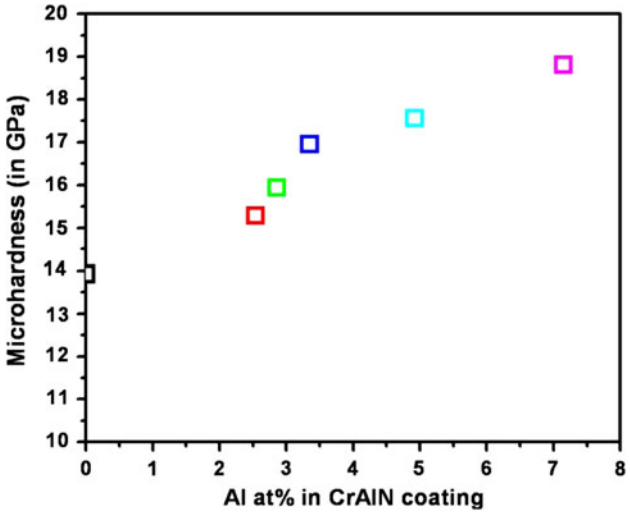

Fig. 6 Microhardness of CrAlN coatings as a function of Al content

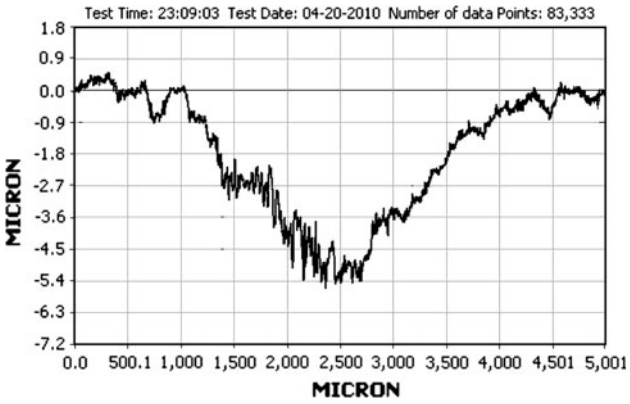

Fig. 7 Wear track produced on counter material (EN32) after CrAlN-coated pin slide over specific time period (test condition: 10 N, 0.5 m/s, 2000 m sliding distance, 30 °C, 32%Rh)

Table 4 Pin-on-disk wear test parameters

Coating	CrN and CrAlN coating
Substrate/pin material	Stainless steel SA304
Counter material (disk)	EN32 (65 HRC)
Normal load applied	10 N
Sliding speed	0.5 m/s
Environment	
Room temperature	28 ± 1 °C
Humidity	32 ± 5%Rh

Figure 8 shows that with lower % of Al content (2.53 at.%), within a around 2.5 to 3 min, the friction forces increases to higher level and with time it is slowly increased to 7.9 N friction force at 66 min sliding distance. Similarly, the CrAlN coating with 2.86 at.% Al content, the friction force versus sliding distance curve follows a same trend as in the case of 2.53 at.% Al content. However, the friction force is drastically increased at 58 min from 4.8 N to the value 7.0 N. Such an immediate change may be either the delamination of films from the substrate or a fragmentation might have occurred between two sliding parts, pin and disc, and at the same instance, substrate is touching the disc causing higher friction force. It can be deduced from the above observation that wear rate is reducing with increase in Al content and it may enhance the tribological properties due to the reduction in mean coefficient of friction to 5.7 from 5.9 N. The intermediate value of Al content (3.35 at.%) in the CrAlN coating further improves the tribological properties, friction force and wear rate, found to be 4.8 N and 1.0 $mm^3/N \cdot m$, respectively. Further increment of Al at.% to 4.92 and 7.15, the friction force is found to be 5.7 and 5.1 respectively, with more consistency observed in the case of highest Al at.% (7.15 at.%) throughout the testing time. In the case of CrAlN-coating, the average friction coefficient is varied from 0.48 to 0.59. The reported coefficient of friction (COF)

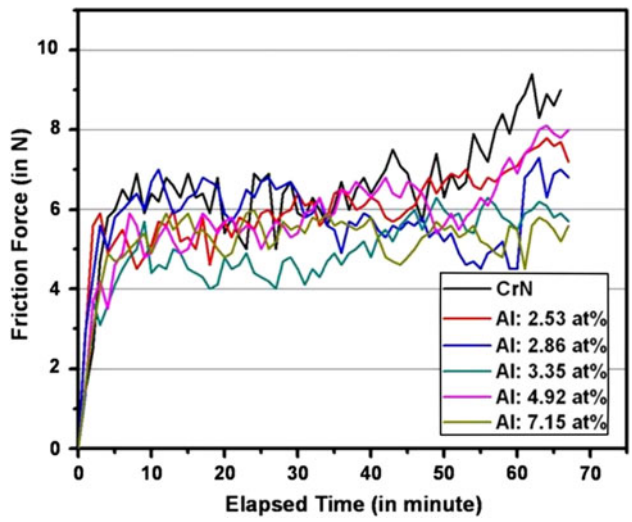

Fig. 8 The friction force produced during CrN- and CrAlN-coated pin slides against its counterpart of EN32 steel (test condition: 10 N, 0.5 m/s, 28 ± 1 °C, 32 ± 5%Rh)

and wear rate are summarized in Table 5. The SEM analysis of the worn out CrAlN-coated pin did not show any transfer of Cr or Al element on the counter material, disk, which indicates better adhesion of coating with the substrate. The results are quite similar to Wang et al. (Ref 24). In addition to the optical photograph, the EDS analyses were performed on the worn coated pin. The EDS result shows mainly Cr, Al, Fe, O, and N elements and hence we presume that the oxides having dark brown in color of Cr, Al, and Fe might have formed (Fig. 9). There is a transfer of material from the counter material, which shows a lower hardness than coating. The counter material (EN32) has worn out strongly than CrN and CrAlN coated pin. The worn particles from counter material, mainly Fe element, oxidize during the tests, which is found as wear debris, get transferred and stick on the surface of the coated pin as shown in Fig. 9. However, the coating material, mainly CrN and CrAlN are not found on counter material, which is confirmed by EDS.

Table 5 Influence of nitrogen content and Al content on coefficient of friction and wear loss of CrN and CrAlN coatings deposited in same condition studied using pin-on-disk method

Samples	Al at.% in the coating	COF (with counter material used steel)	Wear loss $K' \times 10^{-5}$ ($mm^3/N \cdot m$)
CrN	0	0.63	3.5
CrAlN	2.53	0.59	2.5
CrAlN	2.86	0.57	1.5
CrAlN	3.35	0.48	1.0
CrAlN	4.92	0.57	2.0
CrAlN	7.15	0.51	1.0

Wear debris, in general, are composed of the particles spalling from the pin, a stationary part considered as an upper part, and the disc, a dynamically active part having specific sliding velocity considered as a lower specimens during the wear process. In order to understand the correlation between wear debris and wear rate of the specimens, the constituents of the debris should be determined first. The mean particle size is naturally related to operating conditions. In this study, the load applied to wear tests was always constant at 10 N. The micrographs of wear debris reveal that the mean particle size produced at different chemical compositions cannot be used as the standard of evaluating specimen's wear rate as it shows same behavior in CrN and CrAlN coating. The elements of the wear debris generated at the sliding speed of 0.5 m/s are mostly composed of iron and ironic oxides as well as a small amount of hard coating, i.e., CrN particles. As the coated specimens become hard by adding the different elements, i.e., addition of Al and Si in CrN coating, the wear loss of the upper specimen, different coated pins, is no longer the dominant one. However, wear loss of the lower specimen is actually contributed the major part of the debris quantity. During wear test, the transferred materials from the counter material can be compacted and mechanically mixed with the coating material, and the mixture of debris formed a thin layer and stick to the coated surface which contribute to the reduction in wear (Ref 45). Due to the localized high temperature caused by friction during dry sliding, the surface layer also reacted with oxygen in the ambient room atmosphere forming oxides. This tribo-oxidation plays an important role in controlling friction between the sliding pin and disc surface, therefore affecting the wear behavior of the coatings. It is evident from the wear rates shown in Table 5 that the formation of transfer layer in the coating sample with increase in Al content has contributed to the reduced wear rate.

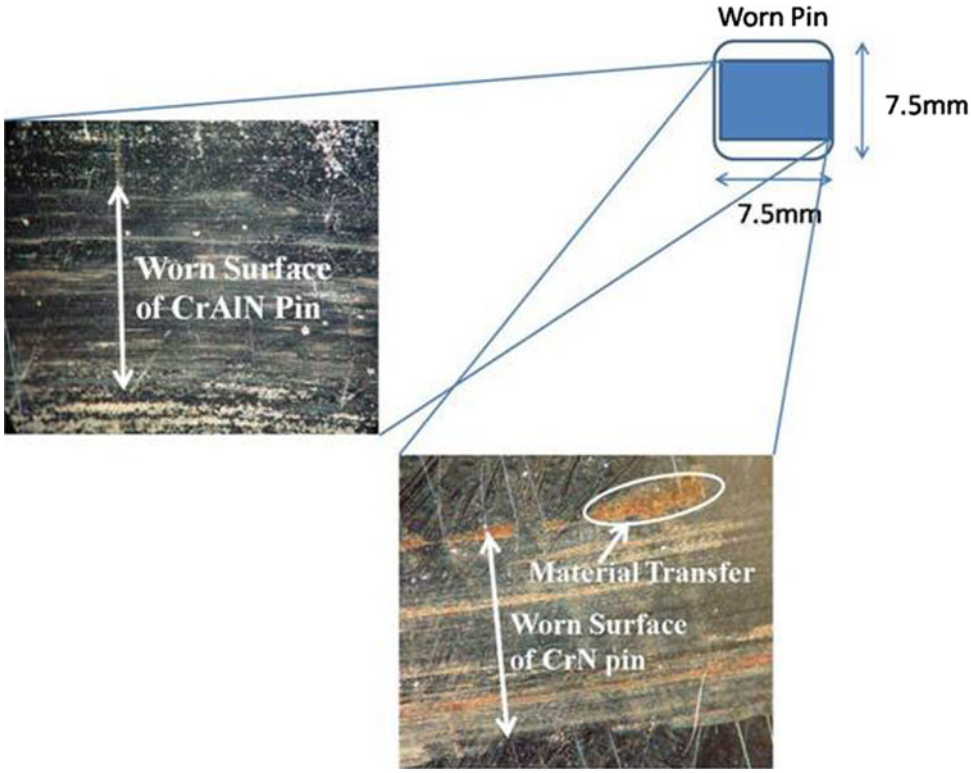

Fig. 9 Optical image of worn out surface of CrN- and CrAlN-coated pin after pin-on-disk test. Arrow indicates the sliding direction (test condition: 10 N, 0.5 m/s, 30 ± 1 °C, 32 ± 5%Rh)

4. Conclusion

CrAlN coatings with different Al contents were deposited on SA304 substrates prepared by a magnetron sputtering technique. The coatings are highly textured with a dominating peak of CrN(111), with its position shifted to higher 2θ angle with increasing Al content deposited on SA304. There is no appreciable peak separation found within the range of applied power to the Al target. The grain size is reduced initially up to 4.92 at.% Al content and then grain size increases with further increase in Al content to 7.15%. The surface roughness is comparatively low, between 6 and 10 nm in all the coatings with varying Al content. The low surface roughness and high density of the coating may be due to increasing applied voltage to Al target, which increases mobility of the atoms and results in higher nucleation density leading to denser coating. The measured microhardness found to be increased with increase in Al content. The minimum and maximum hardness measured were 15.28 and 18.81 GPa, respectively, which is higher than CrN coatings (13.93 GPa) deposited under similar conditions. The wear resistance of all the CrAlN coatings is better than that of pure CrN coating deposited under similar conditions, and the wear resistance is improved gradually with the increase of aluminum incorporation. Wear rate is reduced with increase in Al content and it may enhance the tribological properties as its mean coefficient of friction is reduced to 4.8 in the case of CrAlN coating, while in CrN coating the COF was found to be 0.644.

Acknowledgments

The authors would like to thank Dr. Ramesh Chandra for having provided the PVD facilities for the present work in the nanoscience laboratory. One of the authors, Hetal N. Shah would like to thank Charotar University of Science and Technology, Changa, for granting a study leave to pursue this work.

References

1. M. Kawate, A.K. Hashimoto, and T. Suzuki, Oxidation Resistance of CrAlN and TiAlN Films, *Surf. Coat. Technol.*, 2003, **165**, p 163–167
2. M. Uchida, N. Nihira, A. Mitsuo, K. Toyoda, K. Kubota, and T. Aizawa, Friction and Wear Properties of CrAlN and CrVN Films Deposited by Cathodic Arc Ion Plating Method, *Surf. Coat. Technol.*, 2004, **177–178**, p 627–630
3. J. Romero, M.A. Gómez, J. Esteve, F. Montalà, L. Carreras, M. Grifol, and A. Lousa, CrAlN Coatings Deposited by Cathodic Arc Evaporation at Different Substrate Bias, *Thin Solid Films*, 2006, **515**, p 113–117
4. X.Z. Ding and X.T. Zeng, Structural, Mechanical and Tribological Properties of CrAlN Coatings Deposited by Reactive Unbalanced Magnetron Sputtering, *Surf. Coat. Technol.*, 2005, **200**, p 1372–1376
5. H.C. Barshilia, N. Selvakumar, B. Deepthi, and K.S. Rajam, A Comparative Study of Reactive Direct Current Magnetron Sputtered CrAlN and CrN Coatings, *Surf. Coat. Technol.*, 2006, **201**, p 2193–2201
6. S.R. Pulugurtha and D.G. Bhat, A Study of AC Reactive Magnetron Sputtering Technique for the Deposition of Compositionally Graded Coating in the Cr–Al–N System, *Surf. Coat. Technol.*, 2006, **201**, p 4411–4418
7. T. Li, M. Li, and Y. Zhou, Phase Segregation and its Effect on the Adhesion of Cr–Al–N Coatings on K38G Alloy Prepared by Magnetron Sputtering Method, *Surf. Coat. Technol.*, 2007, **201**, p 7692–7698
8. P.H. Mayrhofer, D. Music, Th Reeswinkel, H.-G. Fuß, and J.M. Schneider, Structure, Elastic Properties and Phase Stability of $Cr_{1-x}Al_xN$, *Acta Mater.*, 2008, **56**, p 2469–2475
9. M. Brizuela, A. Garcia-Luis, I. Braceras, J.I. Oñate, J.C. Sánchez-López, D. Martínez-Martínez, C. López-Cartes, and A. Fernández, Corrosion Resistance of CrAlN and TiAlN Coatings Deposited by Lateral Rotating Cathode Arc, *Surf. Coat. Technol.*, 2005, **200**, p 192–197
10. X.Z. Ding, A.L.K. Tan, X.T. Zeng, C. Wang, T. Yue, and C.Q. Sun, Corrosion Resistance of CrAlN and TiAlN Coatings Deposited by Lateral Rotating Cathode Arc, *Thin Solid Films*, 2008, **516**, p 5716–5720
11. Y. Sun, Y.H. Wang, and H.P. Seow, Effect of Substrate Material on Phase Evolution in Reactively Sputtered Cr-Al-N Films, *J. Mater. Sci.*, 2004, **39**, p 7369–7371
12. Y. Chunyan, T. Linhai, W. Yinghui, W. Shebin, L. Tianbao, and X. Bingshe, The Effect of Substrate Bias Voltages on Impact Resistance of CrAlN Coatings Deposited by Modified Ion Beam Enhanced Magnetron Sputtering, *Appl. Surf. Sci.*, 2009, **255**, p 4033–4038
13. J.E. Sanchéz, O.M. Sanchéz, L. Ipaz, W. Aperador, J.C. Caicedo, C. Amaya, M.A. Hernández Landaverde, F. Espinoza Beltran, J. Muñoz-Saldaña, and G. Zambrano, Mechanical, Tribological, and Electrochemical Behavior of CrAlN Coatings Deposited by r.f. Reactive Magnetron Co-Sputtering Method, *Appl. Surf. Sci.*, 2010, **256**, p 2380–2387
14. Y. Makino and K. Nogi, Synthesis of Pseudobinary CrAlN Films with B1 Structure by rf-Assisted Magnetron Sputtering Method, *Surf. Coat. Technol.*, 1998, **98**, p 1008–1012
15. O. Banakh, P.E. Schmid, R. Sanjine's, and F. Lévy, High-Temperature Oxidation Resistance of CrAlN Thin Films Deposited by Reactive Magnetron Sputtering, *Surf. Coat. Technol.*, 2003, **163–164**, p 57–61
16. S. Ulrich, H. Holleck, J. Ye, H. Leiste, R. Loos, M. Stuber, P. Pesch, and S. Sattel, Influence of Low Energy Ion Implantation on Mechanical Properties of Magnetron Sputtered Metastable (Cr, Al)N Thin Films, *Thin Solid Films*, 2003, **437**, p 164–169
17. M.A. Baker, P.J. Kench, M.C. Joseph, C. Tsotsos, A. Leyland, and A. Matthews, The Nanostructure and Mechanical Properties of PVD CrCu (N) Coatings, *Surf. Coat. Technol.*, 2003, **162**, p 222–227
18. Y.L. Su, S.H. Yao, Z.L. Leu, C.S. Wei, and C.T. Wu, Comparison of Tribological Behavior of Three Films-TiN, TiCN and CrN-Grown by Physical Vapor Deposition, *Wear*, 1997, **213**, p 165–174
19. O. Knotek, F.L. Sffier, and H.-J. Scholl, Properties of Arc-Evaporated CrN and (Cr, Al)N Coatings, *Surf. Coat. Technol.*, 1991, **45**, p 53–58
20. H. Schulz and E. Bergmann, Properties and Applications of Ion-Plated Coatings in the System Cr–C–N, *Surf. Coat. Technol.*, 1991, **50**, p 53–56
21. M.G. Fleming and M.S.J. Hashmi, A Comparison of the Magnetron Sputtered and Arc Evaporated PVD Thin-Films for Wear Applications in Multipoint Cutting Tools, *J. Mater. Process. Technol.*, 1992, **32**, p 481–488
22. R. Wuhrer and W.Y. Yeung, A Comparative Study of Magnetron Co-Sputtered Nanocrystalline Titanium Aluminium and Chromium Aluminium Nitride Coatings, *Scripta Mater.*, 2004, **50**, p 1461–1466
23. S.R. Pulugurtha, D.G. Bhat, M.H. Gordon, J. Shultz, M. Staia, S.V. Joshi, and S. Govindarajan, Mechanical and Tribological Properties of Compositionally Graded CrAlN Films Deposited by AC Reactive Magnetron Sputtering, *Surf. Coat. Technol.*, 2007, **202**, p 1160–1166
24. L. Wang, X. Nie, J. Housden, E. Spain, J.C. Jiang, E.I. Meletis, A. Leyland, and A. Matthews, Material Transfer Phenomena and Failure Mechanisms of a Nanostructured Cr–Al–N Coating in Laboratory Wear Tests and an Industrial Punch Tool Application, *Surf. Coat. Technol.*, 2008, **203**, p 816–821
25. M. Zhou, Y. Makino, M. Nose, and K. Nogi, Phase Transition and Properties of Ti-Al-N Thin Films Prepared by r.f.-Plasma Assisted Magnetron Sputtering, *Thin Solid Films*, 1999, **339**, p 203–208
26. A. Kayani, T.L. Buchanan, M. Kopczyk, C. Collins, J. Lucas, K. Lund, R. Hutchison, P.E. Gannon, M.C. Deibert, R.J. Smith, D.S. Choi, and V.I. Gorokhovsky, Oxidation Resistance of Magnetron-Sputtered CrAlN Coatings on 430 Steel at 800°C, *Surf. Coat. Technol.*, 2006, **201**, p 4460–4466
27. T. Li, Y. Zhou, M. Li, and Z. Li, High Temperature Corrosion Behavior of a Multilayer CrAlN Coating Prepared by Magnetron Sputtering Method on a K38G Alloy, *Surf. Coat. Technol.*, 2008, **202**, p 1985–1993
28. C. Feng, X. Huang, Q. Yang, R. Wei, and D. Nagy, Microstructure and Tribological Properties of CrN and CrSiCN Coatings, *Surf. Coat. Technol.*, 2010, **205**, p 182–188

29. J.C. Sánchez-López, D. Martínez-Martínez, C. López-Cartes, A. Fernández, M. Brizuela, A. García-Luis, and J.I. Oñate, Mechanical Behavior and Oxidation Resistance of CrAlN Coatings, *J. Vac. Sci. Technol. A*, 2005, **23**, p 681–686
30. X.Z. Ding, X.T. Zeng, Y.C. Liu, F.Z. Fang, and G.C. Lim, $Cr_{1-x}Al_xN$ Coatings Deposited by Lateral Rotating Cathode Arc for High Speed Machining Applications, *Thin Solid Films*, 2008, **516**, p 1710–1715
31. B. Tlili, N. Mustapha, C. Nouveau, Y. Benlatreche, G. Guillemot, and M. Lambertin, Correlation Between Thermal Properties and Aluminum Fractions in CrAlN Layers Deposited by PVD Technique, *Vacuum*, 2010, **84**, p 1067–1074
32. S. PalDey and S.C. Deevi, Single Layer and Multilayer Wear Resistant Coatings of (Ti Al)N: A Review, *Mater. Sci. Eng. A*, 2002, **342**, p 58–79
33. P.H. Mayrhofer, C. Mitterer, L. Hultman, and H. Clemens, Microstructural Design of Hard Coatings, *Prog. Mater. Sci.*, 2006, **51**, p 1032–1114
34. H.C. Ong, A.X.E. Zhu, and G.T. Du, Dependence of the Excitonic Transition Energies and Mosaicity on Residual Strain in ZnO Thin Films, *Appl. Phys. Lett.*, 2002, **80**, p 941–943
35. P. Singh and D. Kaur, Influence of Film Thickness on Texture and Electrical and Optical Properties of Room Temperature Deposited Nanocrystalline V_2O_5 Thin Film, *J. Appl. Phys.*, 2008, **103**, p 043507-1–043507-9
36. V. Chawla, R. Jayagnathan, and R. Chandra, Microstructural Characteristics and Mechanical Properties of Magnetron Sputtered Nanocrystalline TiN Films on Glass Substrate, *Bull. Mater. Sci.*, 2009, **32**(2), p 117–123
37. C. Gautier and J. Machet, Study of the Growth Mechanisms of Chromium Nitride Films Deposited by Vacuum ARC Evaporation, *Thin Solid Films*, 1997, **295**, p 43–52
38. J. Pelleg, L.Z. Zevin, S. Lungo, and N. Croitoru, Reactive Sputter Deposited TiN Films on Glass Substrates, *Thin Solid Films*, 1991, **197**, p 117–128
39. N. Schell, J.H. Petersen, J. Bøttiger, A. Mucklich, J. Chevallier, K.P. Andreasen, and F. Eichhorn, On the Development of Texture During Growth of Magnetron-Sputtered CrN *Thin Solid Films*, 2003, **436**, p 100–110
40. E. Lugscheider, K. Bobzin, Th Hornig, and M. Maes, Investigation of the Residual Stresses and Mechanical Properties of (Cr, Al)N arc PVD Coatings Used for Semi-Solid Metal (SSM) Forming Dies, *Thin Solid Films*, 2002, **420–421**, p 318–323
41. L. Cunha, M. Andritschky, K. Pischow, and Z. Wang, Microstructure of CrN Coatings Produced by PVD Techniques, *Thin Solid Films*, 1999, **355–356**, p 465–471
42. J. Lin, J.J. Moore, B. Mishra, M. Pinkas, W.D. Sproul, and J.A. Rees, Effect of Asynchronous Pulsing Parameters on the Structure and Properties of CrAlN Films Deposited by Pulsed Closed Field Unbalanced Magnetron Sputtering (P-CFUBMS), *Surf. Coat. Technol.*, 2008, **202**, p 1418–1436
43. A.B. Cheikh Larbi and B. Tlili, Fretting Wear of Multilayered PVD TiAlCN/TiAlN/TiAl on AISI, 4140 Steel, *Surf. Coat. Technol.*, 2006, **201**, p 1511–1518
44. Q. Luo, Origin of Friction in Running-in Sliding Wear of Nitride Coatings, *Tribol. Lett.*, 2010, **37**, p 529–539
45. Q. Yang, L.R. Zhao, F. Cai, S. Yang, and D.G. Teer, Wear, Erosion and Corrosion Resistance of CrTiAlN Coating Deposited by Magnetron Sputtering, *Surf. Coat. Technol.*, 2008, **202**(16), p 3886–3892